Supplementary Information

Developmental perturbation of Purkinje cell function induces male-biased core and associated autism spectrum disorder–like phenotypes in adulthood

Satoshi Kamijo[1,2], Kei Hori[3], Mikio Hoshino[3], Kazutaka Ikeda[1,4], Hideki Miwa[1,5]*

[1]Department of Neuropsychopharmacology, National Institute of Mental Health, National Center of Neurology and Psychiatry, Kodaira, Tokyo 187-8553, Japan

[2]Department of Physiology, National Medical Defense College, Tokorozawa, Saitama 359-8513, Japan

[3]Department of Biochemistry and Cellular Biology, National Institute of Neuroscience, National Center of Neurology and Psychiatry, Kodaira, Tokyo 187-8502, Japan

[4]Addictive Substance Project, Tokyo Metropolitan Institute of Medical Science, Setagaya, Tokyo 156-8506, Japan.

[5]Division of Bioregulatory Pharmacology, Department of Pharmacology, Iwate Medical University, Yahaba, Iwate 028-3694, Japan

*Corresponding author

Department of Neuropsychopharmacology, National Institute of Mental Health, National Center of Neurology and Psychiatry, Tokyo 187-8553, Japan; Division of Bioregulatory Pharmacology, Department of Pharmacology, Iwate Medical University, Yahaba, Iwate 028-3694, Japan

E-mail: Hideki_Miwa@ncnp.go.jp or miwahid@iwate-med.ac.jp (H.M.)

Table of contents:

1. Supplementary Materials and Methods

2. Supplementary Figures 1-9

3. Supplementary Table 1

Supplementary Material and Methods

Animals

Wild-type C57BL/6J mice were obtained from Japan SLC (Shizuoka, Japan), and homozygous B6.129-Gt(ROSA)26Sor$^{tm1(CAG-CHRM4*,-mCitrine)Ute/J}$ mice (IMSR_JAX: 026219, hereafter referred to as LSL-hM4Di-DREADD-mCitrine mice) were purchased from the Jackson Laboratory (Bar Harbor, ME, USA) (1). The L7-Cre line (IMSR_JAX: 004146) was kindly provided by Dr. Kei Hori (2). Animals were housed in the animal facility of the National Center of Neurology and Psychiatry under a 12-h light/dark cycle (lights on at 8:00 a.m.), with food and water available ad libitum. Animals were group-housed with littermates throughout the behavioral testing period. Both male and female mice were used. All animal procedures were approved by and conducted in accordance with the guidelines of the National Center of Neurology and Psychiatry. All efforts were made to minimize the number of animals used and their suffering.

Genotyping

Genotyping was performed using SYBR Green–based PCR with specific primers for the Cre transgene. The primer sequences are listed in Supplementary Table 1. In more than 80% of the animals, PCR-based genotypes were further confirmed histologically by Purkinje cell-specific mCitrine expression in the cerebellum. Previous studies have reported germline recombination in approximately 5% of offspring from the L7-Cre line (3). However, no animals exhibiting systemic recombination were observed among those examined in this study. It is possible that developmental CNO treatment adversely affected the survival of animals carrying germline recombination.

Developmental inhibition of Purkinje cells

Heterozygous L7-Cre mice were crossed with homozygous LSL-hM4Di-DREADD-mCitrine mice to generate Cre-positive and Cre-negative offspring. Cre-positive offspring are hereafter referred to as L7-Cre; hM4Di mice. Pups of both genotypes received oral administration of clozapine-N-oxide dihydrochloride (CNO, 5 mg/kg, Hello Bio, Bristol, UK) once daily during the designated intervention period (P11-15, P11-20, or P21-30). A 5 μg/mL CNO solution was diluted 1:1 with 80% condensed milk (Morinaga Milk Industry, Tokyo, Japan) in saline to a final CNO concentration of 2.5 μg/mL. For administration, each pup was gently restrained by the dorsal skin, and the CNO solution was delivered directly into the mouth using a P-20 micropipette, following previously described procedures (4).

In vitro slice electrophysiology

Sagittal cerebellar slices (250 μm thickness) containing the deep cerebellar nuclei (DCN) were prepared from L7-Cre; hM4Di mice at postnatal days 15-20, using standard procedures (5). Slices were perfused with a medium that was saturated with 95% O_2 and 5% CO_2 and contained (in mM) 125 NaCl, 2.5 KCl, 2 $CaCl_2$, 1 $MgSO_4$, 1.25 NaH_2PO_4, 26 $NaHCO_3$, and 20 glucose. The medium (at 30 ± 1°C) containing 10 μM 6-cyano-7-nitroquinoxaline-2,3-dione (CNQX) and 25 μM D-(–)-2-amino-5-phosphonovaleric acid (D-APV) was used to record inhibitory postsynaptic currents (IPSCs). Whole-cell patch-clamp recordings were made from large glutamatergic neurons in the DCN with a MultiClamp 700B patch-clamp amplifier (Molecular Devices, Union City, CA, USA). The pipette solution contained (in mM): 122.5 cesium gluconate, 17.5 CsCl, 10 HEPES, 0.2 EGTA, 8 NaCl, 2 Mg-ATP, and 0.3 Na_3-GTP (pH 7.2; 290–310 mOsm). The recording electrodes had resistances of 2–4 MΩ. The series resistance was 10–30 MΩ and was monitored online throughout the experiment. The experiments were rejected if the series resistance changed by more than 20%. The signal was filtered at 5 kHz and digitized at 20 kHz with a National Instruments DAQ board (USB-6341) and Igor Pro (Wavemetrics) with the NeuroMatic software package (6). Synaptic responses were evoked at 0.1 Hz using a bipolar stimulating electrode placed in the white matter fiber tract surrounding the DCN. The cells were voltage-clamped at 0 mV to record IPSCs. Paired-pulse ratio of synaptic responses was measured by delivering afferent fiber stimulation twice at an interstimulus interval of 100 msec. CNQX, D-APV, and CNO were purchased from Tocris Bioscience (Bristol, UK).

Behavioral analyses

A battery of behavioral tests was performed largely as previously described (5), with minor modifications as detailed below. Behavioral testing began at 8 weeks of age. Animals were handled by the experimenter for 5 consecutive days before the first test. Behavioral assays were conducted in the following order: open field test, marble burying test, three-chamber social interaction test, accelerating rotarod test, grooming test, elevated plus maze test, acoustic startle response/prepulse inhibition test, and Barnes maze test.

Open field test

Mice were placed individually in a white square chamber (40 × 40 cm; Maze Engineers, Boston, MA, USA) illuminated at 100 lux, and their behavior was recorded for 15 min

using ANY-maze software (Stoelting, Wood Dale, IL, USA). Average locomotor speed was calculated as total distance traveled divided by time spent moving. The chamber was cleaned with 70% ethanol between trials.

Accelerating rotarod test

Each mouse was placed on a 3.2-cm-diameter rod (RRAC-3002; O'Hara, Tokyo, Japan) rotating initially at 4 rpm. The rotation speed gradually increased to 40 rpm over a 5-min period. Mice underwent four trials per day for 2 consecutive days with 2-h inter-trial intervals. Latency to fall was defined as the time at which the animal fell from the rotarod.

Marble burying test

A semi-transparent plastic chamber (30 × 44 cm), illuminated at 25 lux, was filled with 5 cm of Alpha-dri paper bedding (Shepherd Specialty Papers, Watertown, TN, USA). Green glass marbles (12.5 mm in diameter) were evenly arranged in a 5 × 5 grid on the bedding surface. Each mouse was placed in the chamber for 30 min. Marbles with more than two-thirds of their surface covered by bedding were counted as buried.

Three-chamber social interaction test

Social interaction was assessed using a three-chamber test (7, 8). The apparatus consisted of a rectangular plastic chamber (40 × 60 cm; Maze Engineers, Boston, MA, USA), illuminated at 20 lux. The apparatus was divided into three compartments, with an inverted wire cage placed at each end. The test comprised three 10-min phases. During the habituation phase, the mouse was allowed to explore all three compartments containing empty wire cages. In the pre-test phase, the mouse was habituated to non-social objects (rolled KimWipes) placed in the cages. In the social preference phase, one cage contained an age- and sex-matched unfamiliar C57BL/6J mouse (social stimulus) and the other cage contained a novel wooden block (object stimulus). Animal behavior was automatically tracked using ANY-maze, and the time spent investigating each stimulus was quantified. A social preference index was calculated as:

$$Social\ preference\ index\ = \frac{time_{social} - time_{object}}{time_{social} + time_{object}}$$

The chamber was cleaned with 70% ethanol between phases, and the side of the social stimulus was pseudo-randomly alternated across trials.

Grooming test

Each mouse was placed in an empty plastic cage illuminated at 25 lux and recorded for 10 minutes using a See3CAM_CU55_MHK_TC camera (e-con Systems, Chennai, India). Grooming behavior was defined as sequential rubbing or licking movements progressing from the face to the tail. Total grooming time was manually measured by an experimenter blinded to genotype.

Barnes maze test

The Barnes maze apparatus consisted of a circular plastic platform (89 cm diameter) with 20 evenly spaced holes along the perimeter (Maze Engineers, Boston, MA, USA). Four visual cues were hung from the ceiling. The platform was evenly illuminated at 800 lux and no aversive sound was used. Mice were habituated to the maze and the escape box over 2 days before testing. The behavioral paradigm comprised four phases: learning (days 1–5), probe test (day 6), reversal learning (days 7–9), and reversal probe test (day 10). During learning, each mouse was assigned a fixed goal location. After removal of the start box, mice explored until they entered the escape box or 300 s elapsed. If a mouse failed to locate the box, the experimenter gently guided it inside. Three consecutive trials per day were conducted for 5 days. The escape box was removed for the probe test and the animals were allowed to explore the maze for 180 s. During reversal learning, the goal location was moved to the opposite side; three trials per day were performed for 3 days, followed by a 180-s reversal probe test. Animal behavior was tracked using ANY-maze. Primary latency (the time to first locate the correct goal hole) was recorded as a measure of training performance. For probe tests, the maze was divided into four quadrants (target, opposite, east, west). The target zone comprised the goal hole plus four adjacent holes. Zone investigation times were calculated, and search strategies were classified according to whether animals preferentially explored the old or new target zone in each 60-s segment during the reversal probe test. Strategy switches were defined as transitions between these two search strategies across consecutive segments. Repeated use of the same search strategy across consecutive segments, despite its failure to guide the animal to the new target location, was interpreted as reduced behavioral flexibility

Elevated plus maze test

Anxiety-like behavior was assessed using a custom-built elevated plus maze consisting of two open arms and two closed arms arranged in a plus configuration. Each arm was

the same size (25 cm long × 5 cm wide), and the closed arms had 15-cm-high transparent walls. The maze was elevated 55 cm above the floor, and the central square was illuminated at 70 lux. Each mouse was placed in the center of the maze, and its behavior was recorded for 8 min using ANY-maze. The primary outcome measure was the time spent in the open arms.

Acoustic startle response (ASR) and prepulse inhibition (PPI) test

Each mouse was restrained in a transparent acrylic cylinder and placed in a startle response apparatus (SR4011; O'Hara, Tokyo, Japan). Background white noise was maintained at 65 dB. For the ASR test, 40-ms white noise pulses at nine intensities (70, 75, 80, 85, 90, 95, 100, 110, 120 dB) were presented five times each. ASR was defined as the average peak acceleration in response to the pulse. For the PPI test, a 20-ms prepulse (0, 70, 75, and 80 dB) was presented 100 ms before a 40-ms 120 dB startle stimulus, repeated 10 times per condition. PPI (%) was calculated as:

$$\text{PPI}\ (\%) = 100 \times \left[1 - \frac{\text{ASR amplitude in startle with prepulse trials}}{\text{ASR amplitude in startle alone trials}}\right]$$

Animals whose response to the 120 dB startle stimulus was less than five times their baseline response during no-stimulus (0 dB) trials were excluded from ASR and PPI analyses.

Electroencephalographic (EEG)/electromyographic (EMG) recordings and sleep-wake analysis

Stereotaxic surgery

Mice were anesthetized with 2% isoflurane and secured in a stereotaxic frame. The scalp was incised, and the periosteum was removed. The skull was treated with 3% hydrogen peroxide and etched with phosphoric acid. To record cortical electrical activity, bilateral frontal neocortical EEG stainless screw electrodes (1.0 mm diameter, 2.5 mm length) were placed at AP: +1.5 mm, ML: ±1.0 mm with a ground electrode at AP: −3.5 mm, ML: +1.5 mm and a reference electrode at AP: −5.5 mm, ML: 0.0 mm. Electrodes were soldered to a headmount (Pinnacle Technology, Lawrence, KS, USA; Model 8402). EMG electrodes were placed in the bilateral trapezius muscles. All chronically implanted components were secured with dental cement (Unifast Trad; GC, Tokyo, Japan). Mice were allowed to recover for at least 2 weeks before EEG recording.

EEG/EMG recordings and data analysis

Prior to experiments, mice were tethered and habituated to the recording chamber for 2 days. Continuous EEG/EMG signals were then recorded using a three-channel amplifier (8200-K1-SL; Pinnacle Technology). Signals were amplified 100×, band-pass filtered at 0.5–200 Hz, and digitized at 1 kHz. As previously described (9), sleep-wake states were manually scored in 4 s epochs as follows: An epoch was classified as wakefulness when the EEG showed a desynchronized low amplitude signal together with high muscle tone in the EMG signal. An epoch was classified as non-rapid-eye- movement (NREM) sleep when the EEG signal showed large amplitude, slow synchronized waves, and a low amplitude EMG signal, except for very brief bursts which were considered twitching. An epoch was classified as rapid-eye- movement (REM) sleep when the EEG signal presented a repetitive stereotyped 'sawtooth' pattern in the theta range (4-9 Hz), with an almost flat EMG signal. Epochs with artifacts, such as wake epochs in which the EEG was contaminated by crosstalk from EMG signals or NREM/REM epochs with large amplitude DC shifts were excluded from EEG analyses. Scoring was performed using Sirenia Sleep (Pinnacle Technology), and EEG signals together with scored epochs were exported for further analysis in Python.

Histology

Animals were deeply anesthetized with a mixture of medetomidine (0.75 mg/kg), midazolam (4 mg/kg), and butorphanol (5 mg/kg), then transcardially perfused with phosphate-buffered saline (PBS, pH 7.4), followed by 4% paraformaldehyde in phosphate buffer. Brains were post-fixed in the same fixative overnight at 4°C, then cryoprotected by sequential immersion in 15% and then 30% sucrose in PBS. Cryoprotected brains were sectioned sagittally at 50 μm. Sections were blocked for 2 h at room temperature in phosphate buffer containing 5% normal goat serum, 1% bovine serum albumin (BSA), and 0.3% Triton X-100. Sections were incubated overnight at 4°C with primary antibodies diluted in phosphate buffer containing 1% normal goat serum, 1% BSA, and 0.3% Triton X-100. The following primary antibodies were used: chicken anti-GFP IgY (1:1000, Abcam, Cat# ab13970, RRID: AB_300798), and mouse anti-Calbindin D-28k IgG (1:1000, Swant, Cat# CB300, RRID: AB_10000347). After washing in PBS containing 0.3% Triton X-100, sections were incubated for 1 h at room temperature with the appropriate secondary antibodies: goat anti-chicken IgY H&L (Alexa Fluor 488) (1:1000, Abcam, Cat# ab150169, RRID: AB_2636803), goat anti-chicken IgG antibody, Alexa Fluor 633 conjugated (1:1000, Thermo Fisher Scientific, Cat# A21103, RRID: AB_1500591), and anti-mouse IgG1 (γ1), CF633 antibody

produced in goat (1:1000, Sigma-Aldrich, Cat# SAB4600335, RRID: N/A). Then, they were washed in PBS, counterstained with Hoechst 33342, and mounted with a Mowiol-based mounting medium. Fluorescence images were acquired using FV1000 and SpinSR10 confocal microscopes (Olympus, Tokyo, Japan), and a BZ-X710 fluorescence microscope (Keyence, Osaka, Japan). Sagittal sections were imaged as tiled montages using the BZ-X710 tiling function with a 4× objective. Confocal images were acquired using 10×, 20×, and 40× objectives with 405-, 488-, and 640-nm excitation lasers.

Transcriptomic analyses

RNA sample preparation

CNO (5 mg/kg) was administered once daily from P11 to P15. Four hours after the final dose on P15, animals were euthanized by decapitation. The forebrain and hindbrain were rapidly dissected using a tissue slicer (Zivic Instruments, Pittsburgh, PA, USA). Total RNA was extracted using TRIzol reagent, followed by purification with the PureLink RNA Mini Kit (Thermo Fisher Scientific).

RNA sequencing

Extracted RNA samples were treated with PureLink DNase (Thermo Fisher Scientific) to remove genomic DNA. For each brain region, three biological replicates were prepared for each sex-genotype group. RNA sequencing was performed by Veritas (Tokyo, Japan). For exploratory identification of transcriptional changes, genes meeting the following criteria were selected: $|\log_2 \text{fold change}| > \log_2(1.25)$, unadjusted $P < 0.01$, and $\log_2(\text{counts per million}) > 4$.

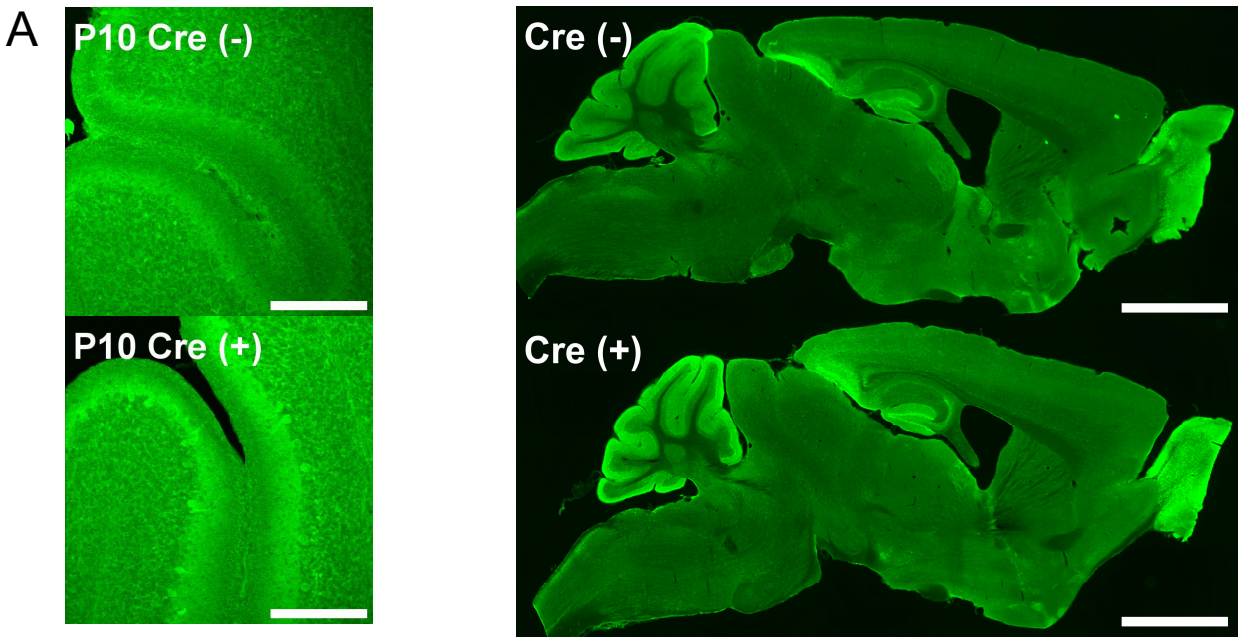
Quantitative RT-PCR

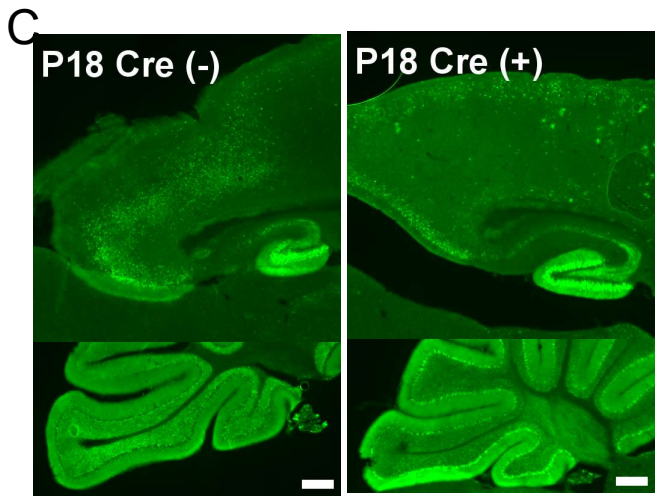
RNA samples were reverse-transcribed using the PrimeScript™ FAST RT Reagent Kit with gDNA Eraser (Takara Bio, Shiga, Japan). Quantitative PCR was performed using the SsoAdvanced™ Universal SYBR® Green Supermix (Bio-Rad, Hercules, CA, USA). Relative gene expression was calculated by the ΔΔCt method. Primer sequences for *Pop4*, *Gabra2*, mCitrine and the reference gene *Ywhaz* are provided in Supplementary Table 1.

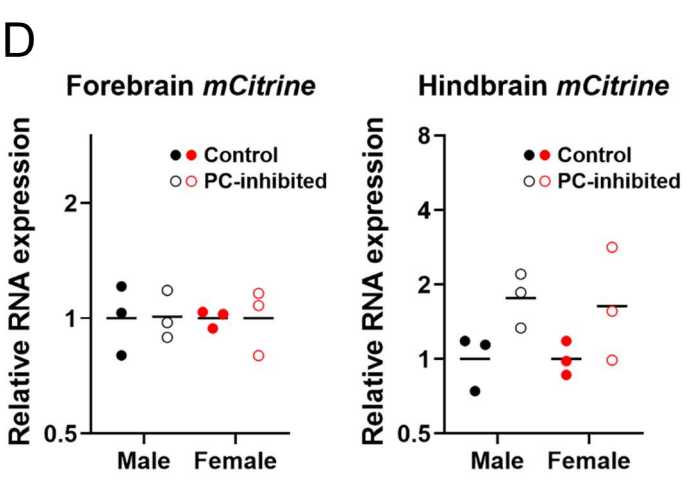
Statistical analyses

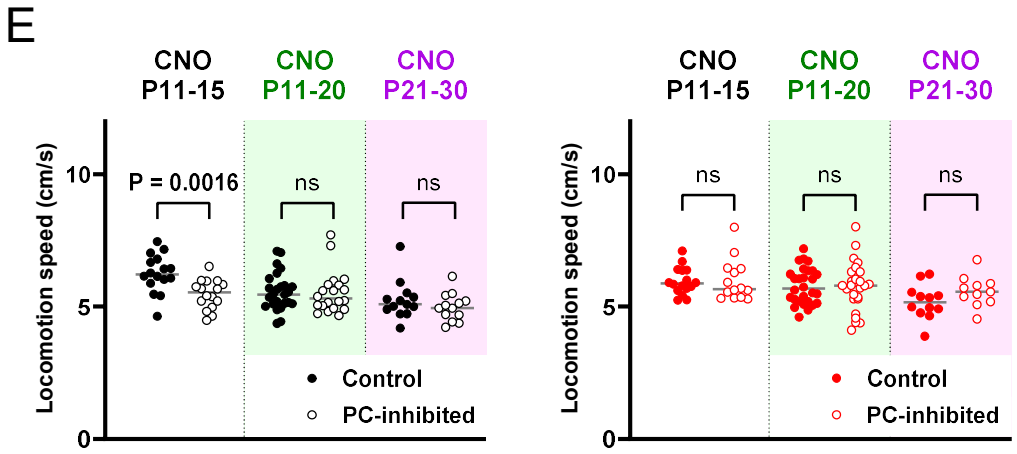
The numbers of mice or replicates used in each experiment are indicated in the individual figure legends. Data are expressed as the mean ± standard error of the mean (SEM) and were analyzed by two-tailed unpaired t-test, or two-way repeated measures

ANOVA, unless otherwise stated. All statistical analyses were performed using GraphPad Prism 10 (GraphPad Software Inc., San Diego, CA, USA) software. P values < 0.05 were accepted as significant. ns, not significant.

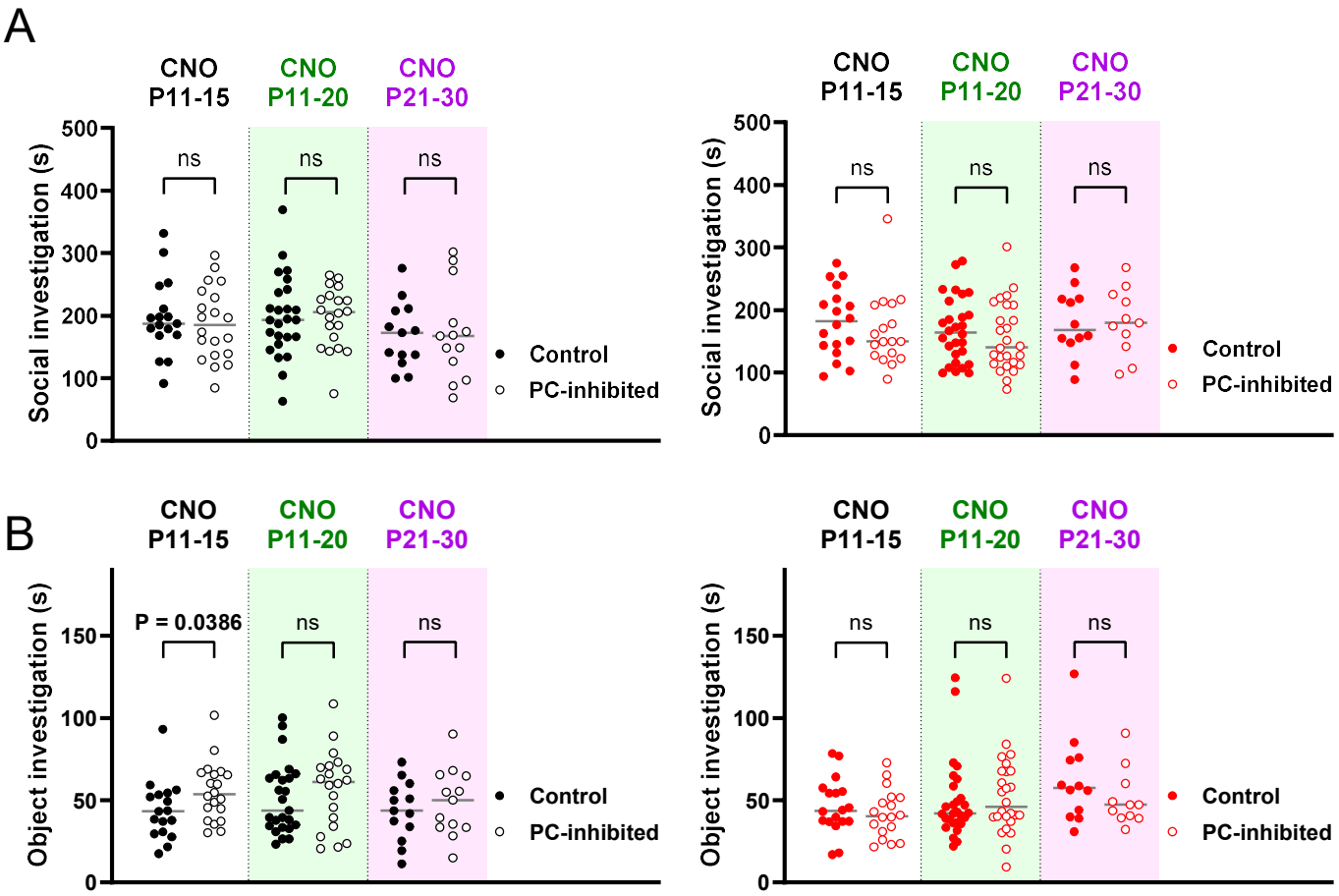

A
P10 Cre (-)
P10 Cre (+)
Cre (-)
Cre (+)


C
P18 Cre (-)
P18 Cre (+)

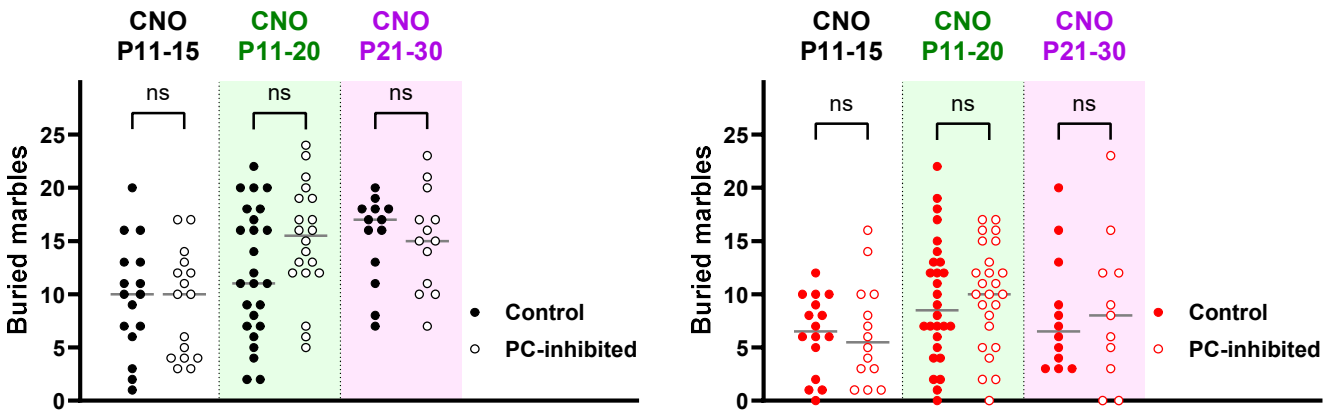

D
Forebrain mCitrine
Hindbrain mCitrine
Relative RNA expression
Control
PC-inhibited
Male
Female


E
CNO P11-15
CNO P11-20
CNO P21-30
Locomotion speed (cm/s)
P = 0.0016
ns
Control
PC-inhibited

Supplementary Figure 1. Brain-wide expression of mCitrine and basic motor performance in PC-inhibited animals. A Native mCitrine fluorescence in the cerebellum of Cre-negative (top) and Cre-positive mice (bottom) at P10. Scale bars, 200 μm. **B** mCitrine expression in sagittal whole-brain sections from adult Cre-negative (top) and Cre-positive (bottom) mice. Scale bars, 2 mm. **C** mCitrine expression in P18 Cre-negative (left) and Cre-positive (right) mice. Hippocampus (top) and cerebellum (bottom). Scale bars, 200 μm. **D** Relative mCitrine mRNA expression levels normalized to control in the forebrain (left, male: 101% [89-118%], female: 100% [80-116%]) and hindbrain (right, male: 176% [133-220%], female: 163% [98-283%]) of P15 mice (N = 3 per condition). Horizontal bars represent geometric means. **E** Locomotor speed (cm/s) in the open field test. Left: male; P11–15 control vs PC-inhibited (N = 16, 16; P = 0.0016); P11–20 (N = 25, 20; P = 0.8554); P21–30 (N = 13, 13; P = 0.2987). Right: female; P11–15 (N = 16, 14; P = 0.9013); P11–20 (N = 28, 26; P = 0.9689); P21–30 (N = 12, 11; P = 0.1371). Data are shown as medians with individual data points. Two-tailed unpaired t-tests were used for statistical comparisons.



Supplementary Figure 2. Social and object investigation time in the three-chamber test. **A** Social investigation time. Left: male; P11–15 control vs PC-inhibited (N = 17, 20; P = 0.6843); P11–20 (N = 25, 20; P = 0.8964); P21–30 (N = 13, 13; P = 0.8798). Right: female; P11–15 (N = 18, 18; P = 0.3271); P11–20 (N = 28, 26; P = 0.3970); P21–30 (N = 12, 11; P = 0.8328). **B** Object investigation time. Left: male; P11–15 control vs PC-inhibited (N = 17, 20; P = 0.0386); P11–20 (N = 25, 20; P = 0.3797); P21–30 (N = 13, 13; P = 0.6866). Right: female; P11–15 (N = 18, 18; P = 0.4292); P11–20 (N = 28, 26; P = 0.4214); P21–30 (N = 12, 11; P = 0.3236). Data are shown as medians with individual data points. Statistical comparisons were performed using two-tailed Mann–Whitney *U* tests.

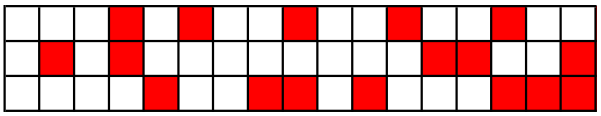


Supplementary Figure 3. Effect of developmental PC inhibition on marble burying behavior. Number of buried marbles. Left: male; P11–15 control vs PC-inhibited (N = 16, 16; P = 0.8741); P11–20 (N = 25, 20; P = 0.1084); P21–30 (N = 13, 13; P = 0.6947). Right: female; P11–15 (N = 16, 14; P = 0.8287); P11–20 (N = 28, 26; P = 0.6292); P21–30 (N = 12, 11; P = 0.9156). Data are shown as medians with individual data points. Statistical comparisons were performed using two-tailed Mann–Whitney *U* tests.

CNO P11-20 male

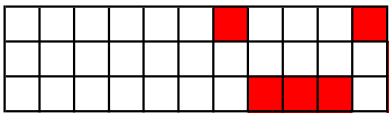
control

0 - 60 s
60 - 120 s
120- 180 s



PC-inhibited

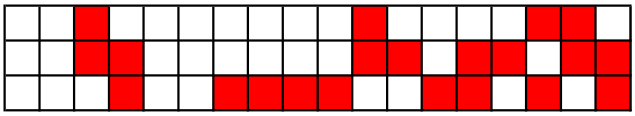
0 - 60 s
60 - 120 s
120- 180 s



CNO P11-20 female

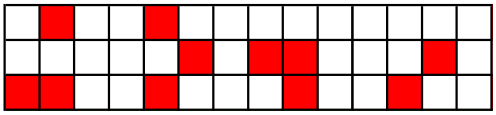
control

0 - 60 s
60 - 120 s
120- 180 s



PC-inhibited

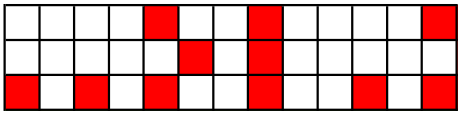
0 - 60 s
60 - 120 s
120- 180 s



CNO P21-30 male

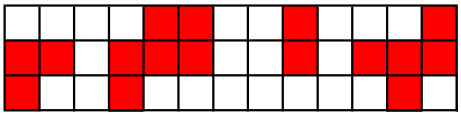
control

0 - 60 s
60 - 120 s
120- 180 s



PC-inhibited

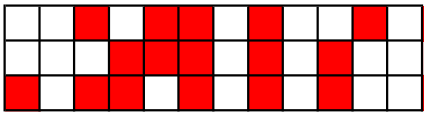
0 - 60 s
60 - 120 s
120- 180 s



CNO P21-30 female

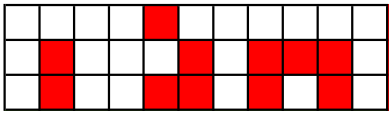
control

0 - 60 s
60 - 120 s
120- 180 s

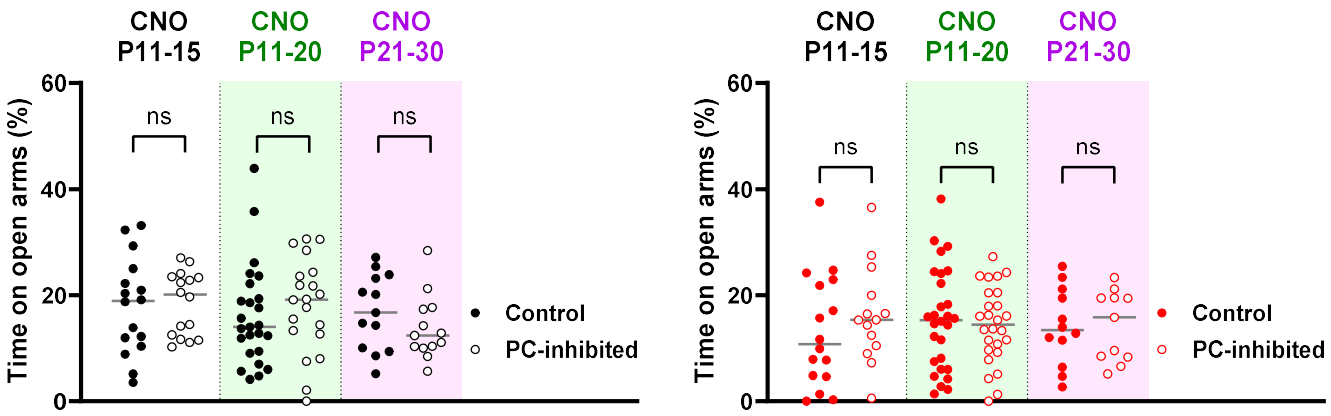


PC-inhibited

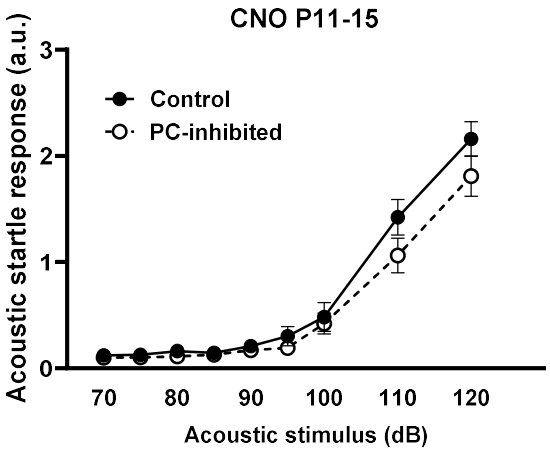
0 - 60 s
60 - 120 s
120- 180 s

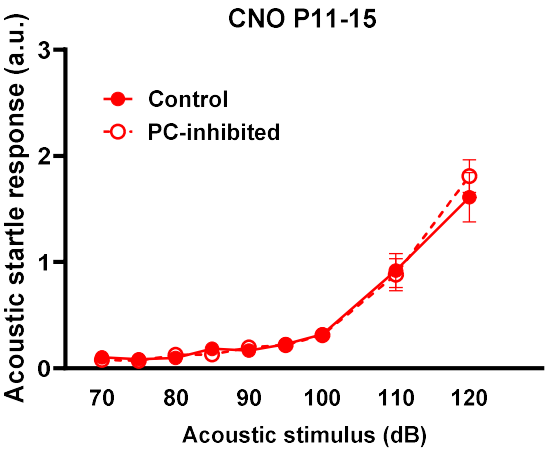


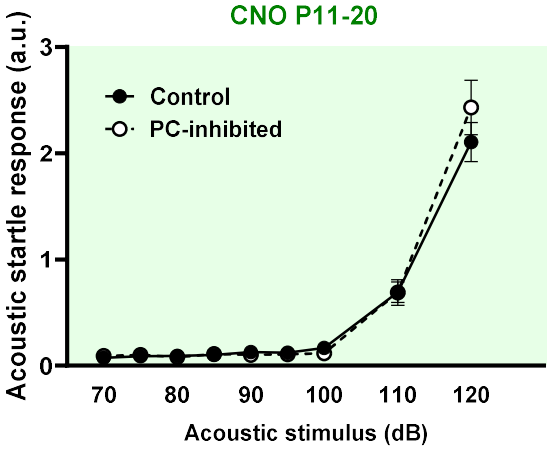
Supplementary Figure 4. Strategy switches of individual animals in the reversal Barnes maze test. Strategies are shown for each mouse across consecutive 60-s segments as white (new goal) or red (old goal). Rows 1-2: P11-20 control vs PC-inhibited males (N = 17, 11); rows 3-4: P11-20 control vs PC-inhibited females (N = 18, 14); rows 5-6: P21-30 control vs PC-inhibited males (N = 13, 13); rows 7-8: P21-30 control vs PC-inhibited females (N = 12, 11). Statistical comparisons of strategy-switch frequencies are presented in Table 1.

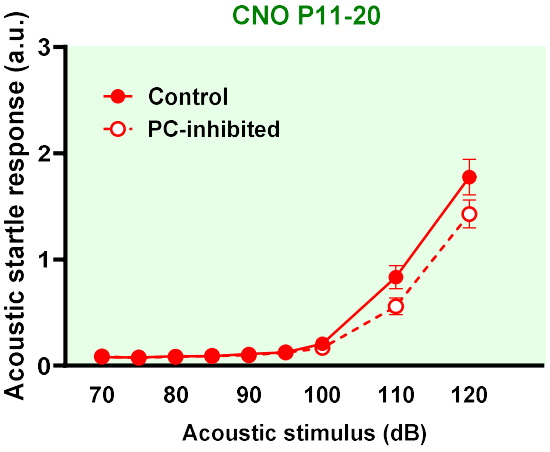


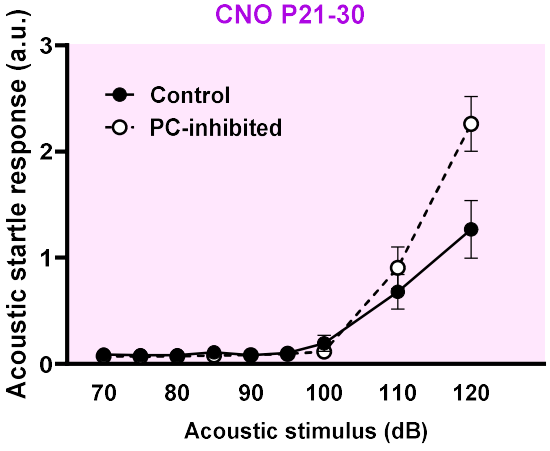
Supplementary Figure 5. Effect of developmental PC inhibition on anxiety-like behavior. Time spent in the open arms of the elevated plus maze. Left: male; P11–15 control vs PC-inhibited (N = 16, 16; P = 0.8526); P11–20 (N = 25, 20; P = 0.4977); P21–30 (N = 13, 13; P = 0.2565). Right: female; P11–15 (N = 16, 14; P = 0.4267); P11–20 (N = 28, 26; P = 0.6595); P21–30 (N = 12, 11; P = 0.9543). Data are shown as medians with individual data points. Statistical comparisons were performed using two-tailed unpaired t-tests.

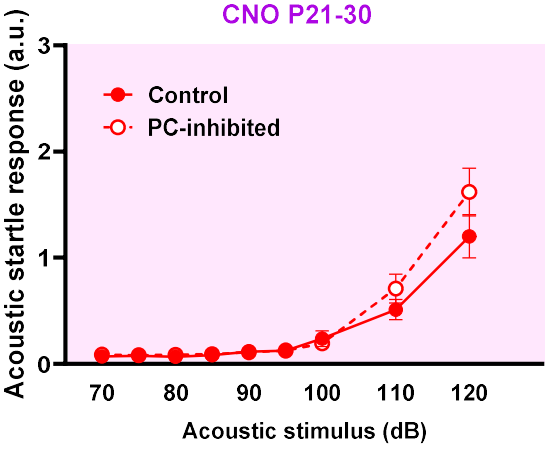

CNO P11-15
Control
PC-inhibited
Acoustic startle response (a.u.)
0
1
2
3
70
80
90
100
110
120
Acoustic stimulus (dB)


CNO P11-15
Control
PC-inhibited
Acoustic startle response (a.u.)
0
1
2
3
70
80
90
100
110
120
Acoustic stimulus (dB)

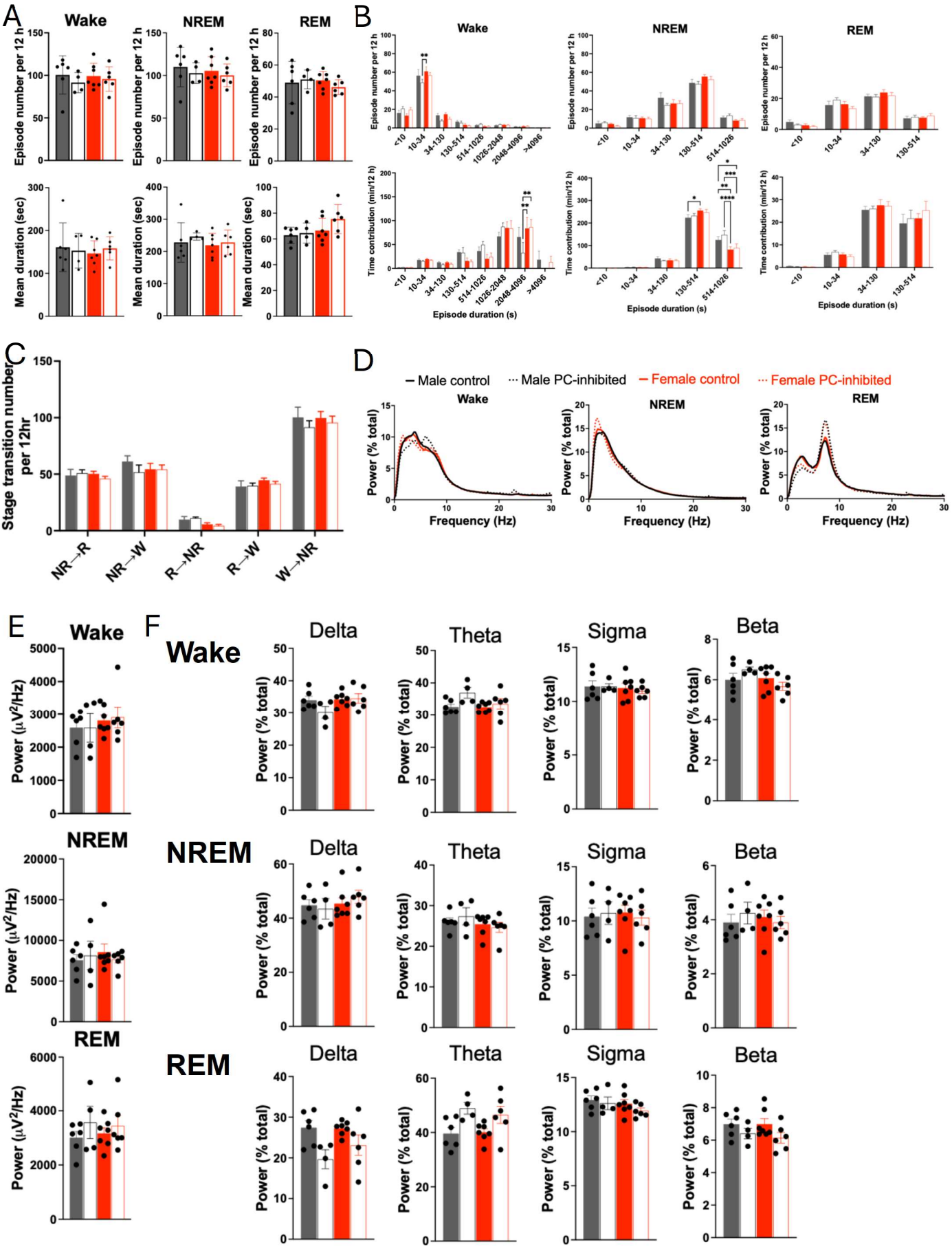

CNO P11-20
Control
PC-inhibited
Acoustic startle response (a.u.)
0
1
2
3
70
80
90
100
110
120
Acoustic stimulus (dB)


CNO P11-20
Control
PC-inhibited
Acoustic startle response (a.u.)
0
1
2
3
70
80
90
100
110
120
Acoustic stimulus (dB)


CNO P21-30
Control
PC-inhibited
Acoustic startle response (a.u.)
0
1
2
3
70
80
90
100
110
120
Acoustic stimulus (dB)


CNO P21-30
Control
PC-inhibited
Acoustic startle response (a.u.)
0
1
2
3
70
80
90
100
110
120
Acoustic stimulus (dB)

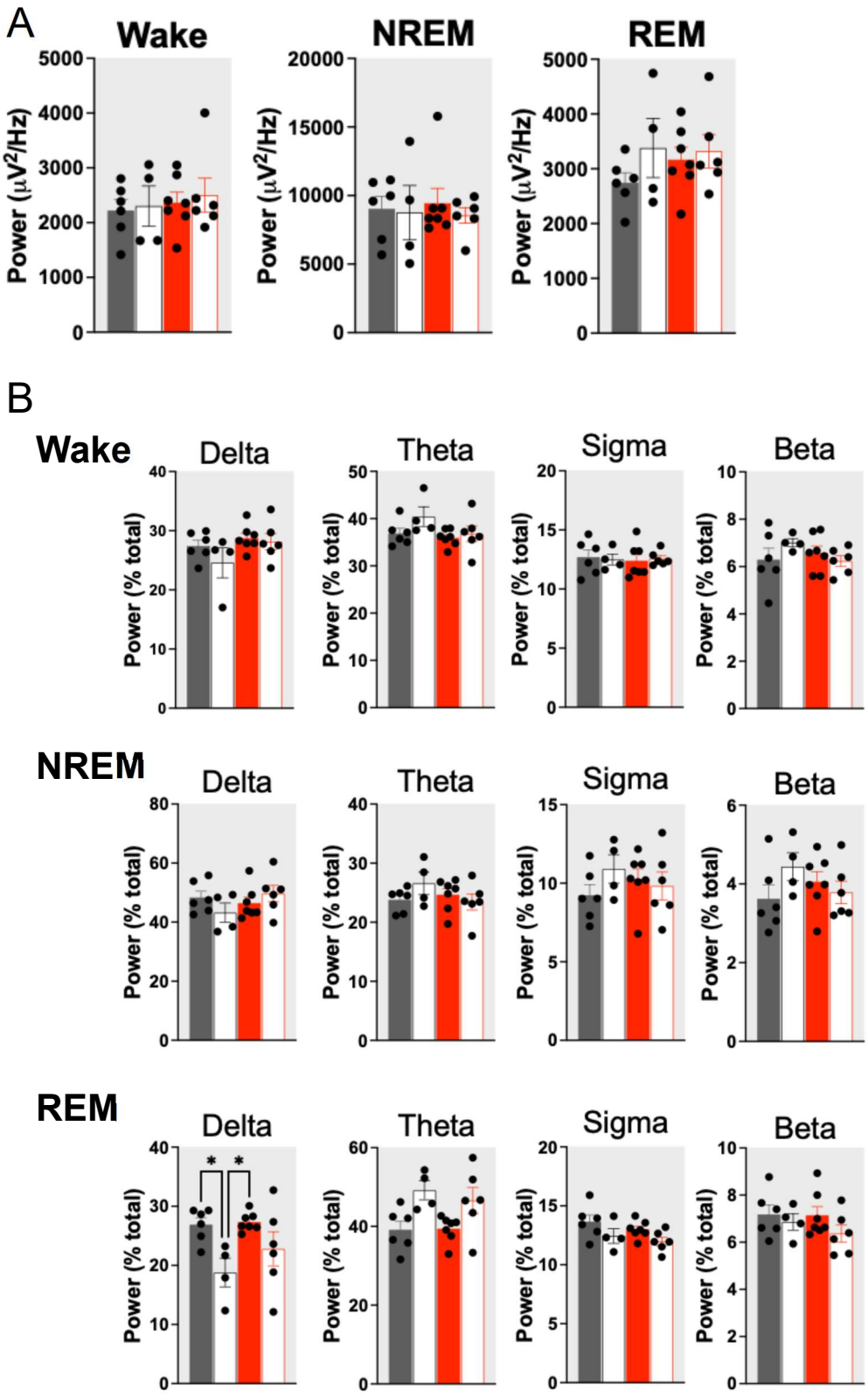
Supplementary Figure 6. Acoustic startle response curves of the tested animals.
Average startle response curves. Top: P11–15 control and PC-inhibited mice (left, male: N = 14, 16; right, female: N = 15, 13). Middle: P11–20 (left, male: N = 24, 19; right, female: N = 25, 23). Bottom: P21–30 (left, male: N = 13, 12; right, female: N = 11, 10). Data are shown as mean ± SEM.


A
Wake
NREM
REM
Episode number per 12 h
Mean duration (sec)
B
Wake
NREM
REM
Episode number per 12 h
Time contribution (min/12 h)
<10
10-34
34-130
130-514
514-1026
1026-2048
2048-4096
>4096
Episode duration (s)
C
Stage transition number per 12hr
NR→R
NR→W
R→NR
R→W
W→NR
D
Male control
Male PC-inhibited
Female control
Female PC-inhibited
Wake
NREM
REM
Power (% total)
Frequency (Hz)
E
Wake
NREM
REM
Power (μV²/Hz)
F
Wake
NREM
REM
Delta
Theta
Sigma
Beta
Power (% total)

Supplementary Figure 7. Sleep–wake architecture and EEG spectral characteristics during the light phase.

A Number (upper) and mean duration (bottom) of wake (left), NREM (middle), and REM (right) episodes during the light phase. Statistical analysis was performed using one-way ANOVA followed by Tukey's multiple comparisons test. One-way ANOVA: episode number, wakefulness, $F(3, 19) = 0.2792$, $P = 0.8397$; NREM sleep, $F(3, 19) = 0.3468$, $P = 0.7919$; REM sleep, $F(3, 19) = 0.3902$, $P = 0.7614$; mean episode duration, wakefulness, $F(3, 19) = 0.1678$, $P = 0.9168$; NREM sleep, $F(3, 19) = 0.3419$, $P = 0.7953$; REM sleep, $F(3, 19) = 2.219$, $P = 0.1191$. **B** Distribution of episode number (upper) and time contributed by episodes within each duration range (bottom) during the light phase. Episode durations were classified as <10, 10–34, 34–130, 130–514, 514–1026, 1026–2048, 2048–4096, and >4096 s. Statistical analysis was performed using two-way ANOVA followed by Tukey's multiple comparisons test. Two-way ANOVA: episode number (top)—wakefulness, duration range, $F(7, 152) = 283.8$, $P < 0.0001$; group, $F(3, 152) = 0.3677$, $P = 0.7764$; interaction, $F(21, 152) = 1.468$, $P = 0.0967$; NREM sleep, duration range, $F(4, 95) = 202.7$, $P < 0.0001$; group, $F(3, 95) = 0.5228$, $P = 0.6677$; interaction, $F(12, 95) = 1.087$, $P = 0.3800$; REM sleep, duration range, $F(3, 76) = 117.6$, $P < 0.0001$; group, $F(3, 76) = 0.4932$, $P = 0.6881$; interaction, $F(9, 76) = 1.011$, $P = 0.4387$; time contribution (bottom)—wakefulness, duration range, $F(7, 152) = 29.63$, $P < 0.0001$; group, $F(3, 152) = 0.1456$, $P = 0.9324$; interaction, $F(21, 152) = 1.252$, $P = 0.2169$; NREM sleep, duration range, $F(4, 95) = 472.6$, $P < 0.0001$; group, $F(3, 95) = 0.7979$, $P = 0.4981$; interaction, $F(12, 95) = 3.126$, $P = 0.0009$; REM sleep, duration range, $F(3, 76) = 144.0$, $P < 0.0001$; group, $F(3, 76) = 0.4410$, $P = 0.7244$; interaction, $F(9, 76) = 0.4496$, $P = 0.9033$. **C** Number of transitions among vigilance states during the light phase. Statistical analysis was performed using two-way ANOVA followed by Tukey's multiple comparisons test. Two-way ANOVA: transition type, $F(4, 95) = 198.3$, $P < 0.0001$; group, $F(3, 95) = 0.6664$, $P = 0.5747$; interaction, $F(12, 95) = 0.4735$, $P = 0.9256$. W: wakefulness, NR: NREM sleep, R: REM sleep. **D** Mean normalized EEG power spectra during wakefulness, NREM sleep, and REM sleep in the light phase. Lines represent group-averaged EEG power spectra; error bars are omitted for clarity. **E** Total EEG power during wakefulness (left), NREM sleep (middle), and REM sleep (right) in the light phase. Statistical analysis was performed using one-way ANOVA followed by Tukey's multiple comparisons test. One-way ANOVA: wakefulness, $F(3, 19) = 0.3457$, $P = 0.7927$; NREM sleep, $F(3, 19) = 0.2512$, $P = 0.8595$; REM sleep, $F(3, 19) = 0.5485$, $P = 0.6552$. **F** Relative EEG power in the delta, theta, sigma, and beta frequency bands (left to right) during wakefulness (top), NREM sleep (middle), and REM sleep (bottom) in the

light phase. Statistical analysis was performed using one-way ANOVA followed by Tukey's multiple comparisons test. One-way ANOVA: wakefulness, delta, $F(3, 19) = 12.055$, $P = 0.1402$; theta, $F(3, 19) = 2.650$, $P = 0.0783$; sigma, $F(3, 19) = 0.2066$, $P = 0.8905$; beta, $F(3, 19) = 1.561$, $P = 0.2317$; NREM sleep, delta, $F(3, 19) = 0.5163$, $P = 0.6760$; theta, $F(3, 19) = 0.7221$, $P = 0.5511$; sigma, $F(3, 19) = 0.09466$, $P = 0.9621$; beta, $F(3, 19) = 0.2915$, $P = 0.8310$; REM sleep, delta, $F(3, 19) = 3.629$, $P = 0.0318$; theta, $F(3, 19) = 3.729$, $P = 0.0291$; sigma, $F(3, 19) = 1.253$, $P = 0.3185$; beta, $F(3, 19) = 1.747$, $P = 0.1914$. Data are presented as mean ± SEM. Male control, N = 6; male PC-inhibited, N = 4; female control, N = 7; female PC-inhibited, N = 6. Statistical tests are indicated for each analysis above. Multiple comparisons were performed using Tukey’s multiple-comparisons test.


A
Wake
NREM
REM
Power (μV²/Hz)
B
Wake
NREM
REM
Delta
Theta
Sigma
Beta
Power (% total)
*
*

Supplementary Figure 8. EEG spectral power during the dark phase.

A Total EEG power during wakefulness (left), NREM sleep (middle), and REM sleep (right) in the dark phase. Statistical analysis was performed using one-way ANOVA followed by Tukey's multiple comparisons test. One-way ANOVA: wakefulness, $F(3, 19) = 0.2237$, $P = 0.8787$; NREM sleep, $F(3, 19) = 0.1369$, $P = 0.9368$; REM sleep, $F(3, 19) = 0.9056$, $P = 0.4568$. **B** Relative EEG power in the delta, theta, sigma, and beta frequency bands (left to right) during wakefulness (top), NREM sleep (middle), and REM sleep (bottom) in the dark phase. Statistical analysis was performed using one-way ANOVA followed by Tukey's multiple comparisons test. One-way ANOVA: wakefulness, delta, $F(3, 19) = 1.615$, $P = 0.2192$; theta, $F(3, 19) = 1.823$, $P = 0.1772$; sigma, $F(3, 19) = 0.07551$, $P = 0.9724$; beta, $F(3, 19) = 0.8639$, $P = 0.4769$; NREM sleep, delta, $F(3, 19) = 1.033$, $P = 0.4006$; theta, $F(3, 19) = 1.068$, $P = 0.3861$; sigma, $F(3, 19) = 0.7334$, $P = 0.5449$; beta, $F(3, 19) = 1.091$, $P = 0.3770$; REM sleep, delta, $F(3, 19) = 4.028$, $P = 0.0225$; theta, $F(3, 19) = 4.249$, $P = 0.0186$; sigma, $F(3, 19) = 2.651$, $P = 0.0782$; beta, $F(3, 19) = 1.045$, $P = 0.3956$. Data are presented as mean ± SEM. Male control, N = 6; male PC-inhibited, N = 4; female control, N = 7; female PC-inhibited, N = 6. $P < 0.05$ was considered statistically significant. P values are indicated as $*P < 0.05$.

Hindbrain DEGs by PC inhibition	Male	Female
Upregulated	*gabra2, pop4, pglyrp1, itgbl1, paxbp1*	*pde8b, zmat5, nol3*
Downregulated	*olig2, zcchc12, fxyd5, stxbp6, etv6, gng4, lor, fxyd7, fhod3*	*fbxl14, arsa, zfp938, vps37b, axin1, ankrd52, cdc42bpg*

Forebrain DEGs by PC inhibition	Male	Female
Upregulated	*gabra2, pop4, eml2, hbb-bs*	*usp9x, sec61a2, thsd7a, nufip2, tenm3, robo1, elavl2*
Downregulated	*kptn*	*ptgds, vasp, bmyc, sf3a2, rpp25, npy, med17, fdxr, plekhj1, gatb, setd1a*

Supplementary Figure 9. Candidate sex-specific differentially expressed genes. Top: candidate DEGs in the hindbrain (left: male, right: female), Bottom: candidate DEGs in the forebrain (left: male, right: female). Genes were selected using the following criteria: (1) $|\log_2(\text{fold change})| > \log_2(1.25)$, (2) Unadjusted P value < 0.01, (3) $\log_2(\text{counts per million}) > 4$.

Supplementary Table 1. Primers used for genotyping and RT-qPCR (5' to 3')

Primer	Sequence (5′–3′)
Cre-fw	ACCTGAAGATGTTCGCGATTATCT
Cre-rv	ACCGTCAGTACGTGAGATATCTT
Pop4-fw	AAGGCTGCCATTTACCATGC
Pop4-rv	TCATGTGAGGTATGCTCTGCT
Gabra2-fw	ACAAAAAGAGGATGGGCTTG
Gabra2-rv	TCATGACGGAGCCTTTCTCT
mCitrine-fw	CGGCGACGTAAACGGCCACAAGTTCAG
mCitrine-rv	CTTGCCGGTGGTGCAGATGAA
Ywhaz-fw	CAGAAGACGGAAGGTGCTGAGA
Ywhaz-rv	CTTTCTGGTTGCGAAGCATTGGG

References

1. Zhu H, Aryal DK, Olsen RH, Urban DJ, Swearingen A, Forbes S, et al. Cre-dependent DREADD (Designer Receptors Exclusively Activated by Designer Drugs) mice. Genesis. 2016;54(8):439-46.
2. Barski JJ, Dethleffsen K, Meyer M. Cre recombinase expression in cerebellar Purkinje cells. Genesis. 2000;28(3-4):93-8.
3. Tsai PT, Hull C, Chu Y, Greene-Colozzi E, Sadowski AR, Leech JM, et al. Autistic-like behaviour and cerebellar dysfunction in Purkinje cell Tsc1 mutant mice. Nature. 2012;488(7413):647-51.
4. Schalbetter SM, Mueller FS, Scarborough J, Richetto J, Weber-Stadlbauer U, Meyer U, et al. Oral application of clozapine-N-oxide using the micropipette-guided drug administration (MDA) method in mouse DREADD systems. Lab Anim (NY). 2021;50(3):69-75.
5. Fujihara K, Miwa H, Kakizaki T, Kaneko R, Mikuni M, Tanahira C, et al. Glutamate Decarboxylase 67 Deficiency in a Subset of GABAergic Neurons Induces Schizophrenia-Related Phenotypes. Neuropsychopharmacology. 2015;40(10):2475-86.
6. Rothman JS, Silver RA. NeuroMatic: An Integrated Open-Source Software Toolkit for Acquisition, Analysis and Simulation of Electrophysiological Data. Front Neuroinform. 2018;12:14.
7. Yang M, Silverman JL, Crawley JN. Automated three-chambered social approach task for mice. Curr Protoc Neurosci. 2011;Chapter 8:Unit 8.26.
8. Rein B, Ma K, Yan Z. A standardized social preference protocol for measuring social deficits in mouse models of autism. Nat Protoc. 2020;15(10):3464-77.
9. Chen L, McKenna JT, Leonard MZ, Yanagawa Y, McCarley RW, Brown RE. GAD67-GFP knock-in mice have normal sleep-wake patterns and sleep homeostasis. Neuroreport. 2010;21(3):216-20.